Energy efficiency assessment of integrated and nonintegrated solar ponds

Ismail Bozkurt[1], Mehmet Karakilcik[1]* and Ibrahim Dincer[2]

[1]Department of Physics, Faculty of Sciences and Letters, University of Çukurova, Adana 01330, Turkey; [2]Faculty of Engineering and Applied Science, University of Ontario Institute of Technology (UOIT), 2000 Simcoe Street, North Oshawa, Ontario, Canada L1H 7K4

Abstract

In this study, an experimental investigation of temperature distribution and efficiencies in conventional solar pond (SP) and integrated SP (ISP) systems is presented. Several temperature-measuring sensors connected to a data acquisition system are used to measure the temperature changes with respect to time and position. In addition, the monthly stored energies of SP and ISP are determined. The maximum and the minimum energy efficiencies of the SP and ISP are observed for the months of August as 28.41 and 33.55% and January as 8.28 and 9.48%, respectively. These then confirm that the SP storage efficiency can be increased by integrating the system with solar collectors.

Keywords: integrated solar pond; solar collector; heat storage performance; energy efficiency

*Corresponding author. ismail_bozkurt44@yahoo.com, kkilcik@cu.edu.tr

Received 30 January 2012; revised 6 March 2012; accepted 9 May 2012

1 INTRODUCTION

Due to increasing local and global energy and environment problems, there has been an increasing interest in renewable energy sources, particularly solar energy, which can be utilized for the production of various output commodities, including power, heat, hot water, cooling and fresh water.

Solar radiation constitutes a vast energy source which is abundantly available in almost all parts of the earth. Solar energy in many regards is one of the best alternatives to nonrenewable sources of energy. One way to collect and store solar energy is through the use of solar ponds (SPs). They can be employed to supply thermal energy for various applications, such as process and space heating, water desalination, refrigeration, drying and power generation [1, 2]. A salinity gradient SP is an integral collection and storage device of solar energy. By the virtue of having built-in thermal energy storage, it can be used irrespective of time and season. In an ordinary pond or lake, when the sun's rays heat up the water, this heated water being lighter, rises to the surface and loses its heat to the atmosphere. This causes the pond water to remain at nearly atmospheric temperature. The SP technology inhibits this phenomenon by dissolving salt into the bottom layer of the pond, making it too heavy to rise to the surface, even when temperatures are high. The salt concentration increases with depth, thereby forming a salinity gradient. The sunlight, which reaches to the bottom of the pond, remains entrapped in storage zone. The useful thermal energy is then withdrawn from the SP in the form of hot brine [3]. Recently, there has been increasing interest in environmentally benign and sustainable energy sources, e.g. solar energy. In this regard, SPs and collectors have received a great attention for their implementation. In the literature, a plethora studies have been undertaken on SPs and solar collectors by various researchers [e.g. 4–16]. Some researchers have also studied integrated systems, e.g. [17–22]. However, there have not been any experimental analyses on comparison of the integrated and non-ISP based on energy efficiency. This is the main motivation behind the present work.

The experimental work presented in this article appears to be original with the idea of integrating the SPs and conducting energy analysis and efficiency assessment of the ISP and non-ISP, and aims to analyze the energy efficiencies for both cases and compare for every month of the year. In this regard, density and temperature distributions in the ISP and collector system are measured and presented.

2 EXPERIMENTAL APPARATUS AND PROCEDURE

Generally, SPs are used to collect and store the thermal energy converted from solar energy. The solar energy is renewable and

International Journal of Low-Carbon Technologies 2014, 9, 45–51
© The Author 2012. Published by Oxford University Press.
This is an Open Access article distributed under the terms of the Creative Commons Attribution Non-Commercial License (http://creativecommons.org/licenses/by-nc/3.0/), which permits non-commercial re-use, distribution, and reproduction in any medium, provided the original work is properly cited. For commercial re-use, please contact journals.permissions@oup.com
doi:10.1093/ijlct/cts052 Advance Access Publication 19 June 2012

Downloaded from https://academic.oup.com/ijlct/article/9/1/45/665396 by Cukurova University user on 05 February 2022

boundless. These systems work at low efficiencies because of the large heat transfer losses. Some of the parameters that affect the system perfromance are shading effect, salty diffusion, heat losses from side and bottom walls as well as the upper surface to air. This system integrates solar flat-plate collector technology to SP technology. The system was built at Space Sciences and Solar Energy Research and Application Center, Cukurova University in Adana, Turkey (i.e. 35°18′ E longitude, 37°05′ N latitude). In this study, we measure density and temperature to determine the energy efficiency and compare it with the energy efficiency of the SP and the ISP. As seen in Figure 1, a novel SP system is called an ISP, which consists of a cylindiric SP with a radius of 0.80 m and a depth of 2 m and four solar collectors with dimensions of 1.90 × 0.90 m.

First, the cylindric SP in the integrated system is composed of three zones. The first zone, upper convective zone (UCZ), is the fresh water layer at the top of the pond. This zone is fed with fresh water to maintain its density as close as possible to the density of fresh water in the upper part and to meet the water loss due to evaporation. The second zone is the nonconvective zone (NCZ) between the heat storage zone (HSZ) and the UCZ. The NCZ is composed of salty water layers whose brine density gradually increases toward HSZ. NCZ plays a key role in workings of a SP. The third zone is the lower convective zone, which is also known as the HSZ. It is composed of salty water with highest density. The high amount of the solar energy is absorbed and stored by this bottom region. Secondly, flat-plate solar collectors are connected to the heat exchanger to transfer heat energy to the SP. These are the most common solar collectors used in solar water-heating systems in homes and space heating systems. The flat-plate collector consists of an insulated metal box with a glass cover and a dark-colored absorber plate. Solar radiation is absorbed by the absorber plate and transferred to a fluid that circulates through the collector in tubes. In an air-based collector, the circulating fluid is air, whereas, in a liquid-based collector, it is usually water. The flat-plate collectors have the advantages of collecting the heat energy very rapidly compared with SPs. Therefore, collected energy using flat-plate collectors can be lost if it is not utilized within a few days. On the other hand, SP can store the thermal energy for a long-term storage.

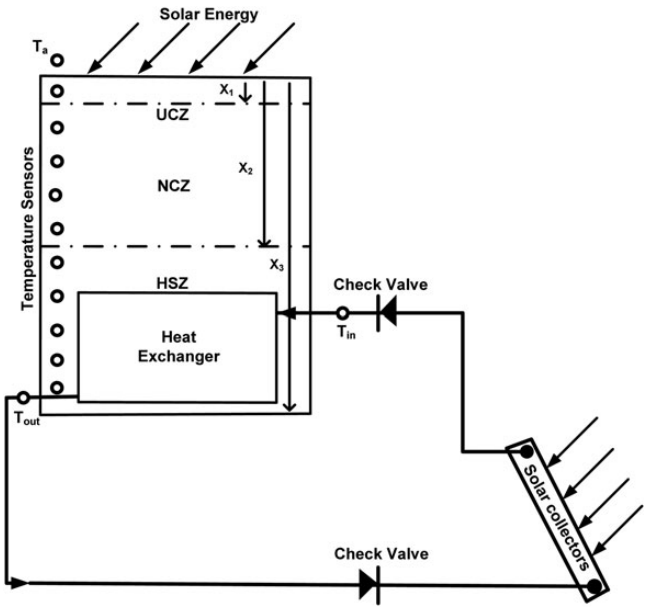


Figure 1. *A schematic view of the ISP.*

Figure 1 shows a schematic representation of an integrated system, consisting of the cylindric SP, heat exchanger and solar collectors. Its experimental temperature distributions were measured using temperature sensors. These sensors were placed into the inner zones as well as the inlet and outlet of the heat exchanger. Hence, the temperature distribution profiles of these regions at any time were experimentally measured by a data acquisition system. To measure the temperature distributions of various regions, the temperature sensors were placed into the inner zones, starting from the bottom, at 0.10, 0.30, 0.50, 0.70, 0.90, 1.10, 1.30, 1.50, 1.70 and 1.90 m heights. The data acquisition system was connected to a computer for data recording, monitoring and processing. The temperatures of the inner layers of the pond, air and input–output of the heat exchanger were measured on an hourly basis throughout the months.

3 ENERGY ANALYSIS

It is very important to determine the amount of stored thermal energy. However, this is generally complicated due to the differences of inner and outer parameters (e.g. pond dimensions, salt water solutions, insulation, zone thicknesses, shading area of the layers, transmission and absorption characteristics for the layers). Here, we consider the following key parameters: the temperatures in the SP and the incident radiation reaching the surface of the pond and collectors. To calculate the heat stored by SP and ISP, the temperature distribution of the zones are measured. The temperature variations of layers depending on incident solar radiation on the horizontal surface, rates of absorption by the layers, local climate conditions, pond structure, time and insulation specifications are used. Temperature distributions of our system were obtained, experimentally. The part of the solar radiation falling on the SP is transmitted through the UCZ and NCZ, after attenuation, to the HSZ. The part of the transmitted solar radiation from the NCZ to the HSZ is reflected from the bottom, and the majority of the solar radiation is absorbed in the HSZ. Therefore, the HSZ temperature increases and a temperature gradient is developed in these zones. The radiation heat losses of the SP are neglected because SPs are working at low temperature. Furthermore, the convection heat losses from the SP are prevented by NCZ, so these heat losses are not considered in the following equations. The energy efficiency of the HSZ of the SP can be defined as:

$$\eta_{SP} = \frac{Q_{st}}{Q_{in}} = 1 - \frac{Q_{bt} + Q_{up} + Q_{side}}{Q_{solar,\,HSZ}} \qquad (1)$$

where Q_{st} is the stored heat energy in the HSZ of the SP. Q_{in} is the amount of net solar energy absorbed by the HSZ, which is

Downloaded from https://academic.oup.com/ijlct/article/9/1/45/665396 by Cukurova University user on 05 February 2022

coming from the sun (represented by $Q_{\text{solar, HSZ}}$). Q_{bt} is the total heat loss to the bottom wall from the HSZ, and Q_{up} is the heat loss from the HSZ to the above zone. Q_{side} is the total heat loss to the side walls of the HSZ. Substituting eqautions for each parameter in Equation (1) provides us with the following energy efficiency of the SP:

$$\eta_{\text{SP}} = \frac{1-(k_{\text{w}}A/\Delta x_{\text{bt}})(T_{\text{bt}}-T_{\text{a}})+(k_{\text{s}}A/\Delta x_{\text{HSZ-NCZ}})(T_{\text{HSZ}}-T_{\text{NCZ}}) + (k_{\text{w}}2\pi rL_{\text{HSZ}}/\Delta x_{\text{side}})(T_{\text{HSZ}}-T_{\text{a}})}{\beta EA_{\text{HSZ}}[(1-F)h(x_3-\delta)]} \quad (2)$$

Flat-plate collectors are connected to increase the performance of the SP. The installation of these flat plate collectors leads to the higher temperature gradient developed in the zone. The general energy efficiency of the HSZ of the ISP can be defined as

$$\eta_{\text{ISP}} = \frac{Q_{\text{st,ISP}}}{Q_{\text{fpc}}+Q_{\text{in}}} = 1-\frac{Q_{\text{bt}}+Q_{\text{up}}+Q_{\text{side}}}{Q_{\text{fpc}}+Q_{\text{solar,HSZ}}} \quad (3)$$

where $Q_{\text{st,ISP}}$ is the stored thermal energy in the HSZ of the ISP. Q_{fpc} is the incident solar energy of the absorber flat-plate surface. Substituting equations for each parameter in Equation (1) provides us with the following thermal energy efficiency (η_{ISP}) of the SP:

$$\eta_{\text{ISP}} = \frac{1-(k_{\text{w}}A/\Delta x_{\text{bt}})(T_{\text{bt}}-T_{\text{a}})+(k_{\text{s}}A/\Delta x_{\text{HSZ-NCZ}})(T_{\text{HSZ}}-T_{\text{NCZ}}) + (k_{\text{w}}2\pi rL_{\text{HSZ}}/\Delta x_{\text{side}})(T_{\text{HSZ}}-T_{\text{a}})}{E(\tau\alpha)A_{\text{fpc}}+\beta EA_{\text{HSZ}}[(1-F)h(x_3-\delta)]} \quad (4)$$

where m is the mass of hot water supplied to the SP through heat exchanger, the flat-plate collectors. C is the specific heat capacity, E is the total solar energy reaching the SP surface, A_{HSZ} is the area of the HSZ, which is subjected to solar insolation, F is the fraction of energy absorbed at a region of δ-thickness, h is the solar radiation ratio; A is the surface area of the SP, T_{a} is the ambient air temperature, k_{w} is the thermal conductivity of the side and bottom walls, k_{s} is the thermal conductivity of the salty water, L_{HSZ} is the thickness of the HSZ (m), r is the inner radius of the cylindiric SP, Δx_{bt} is the thickness of the bottom wall, Δx_{side} is the thickness of the side wall, $\Delta x_{\text{HSZ-NCZ}}$ is the thickness of the HSZ's middle point and the NCZ's middle point, A_{fpc} is the collector area, τ is the transmission coefficient of the collector surface, α is the emissivity of the absorber surface of the flat plate collector and β is the fraction of the incident solar radiation that actually enters the pond and is given by [23].

$$\beta = 1-0.6\left[\frac{\sin\theta_{\text{i}}-\sin\theta_{\text{r}}}{\sin\theta_{\text{i}}+\sin\theta_{\text{r}}}\right]^2-0.4\left[\frac{\tan\theta_{\text{i}}-\tan\theta_{\text{r}}}{\tan\theta_{\text{i}}+\tan\theta_{\text{r}}}\right]^2$$

where θ_{i} and θ_{r} are the incidence and refraction angles. h represents the ratio of the solar energy reaching the depth in the layer I to the total solar incident falling on to the surface of the pond and is given by Bryant and Colbeck [24] as $h_I = 0.727 - 0.056\ln[(x_I-\delta)/\cos\theta_{\text{r}}]$ (here x_{I} is the thickness of the layer, δ; thickness of the layer in the UCZ where long-wave solar energy is absorbed).

4 RESULTS AND DISCUSSION

A SP is used to store the heat energy in the first experiment. The amount of heat stored by the SP is calculated throughout the year. The first experiment, which is carried out to store the thermal energy by using conventional SP, is conducted in the winter to store the thermal energy. In the second experiment, ISP system is used to store much more heat energy for the same winter period. As a result, the HSZ of the conventional SP stores much more thermal energy if flat-plate collectors are used especially in winter months. The considerable energy efficiency increase is obtained by using collectors. Solar collectors significantly affect the thermal performance of the SP. The average monthly thermal energy storage has been found to be increased considerably while the SP is integrated with solar collectors. The simplicity as well as the environmental and economic advantages of ISP with solar collectors compensate for the disadvantages in the efficiency of the non-ISP. As a result, low energy efficiency of the conventional SP is increased by using solar collectors.

Figure 2 shows the variations of the experimentally measured salty water densities with respect to the height measured from the bottom of the ISP throughout the year. Some slight differences are observed between the densitities due to increase of the inner zone temperature and diffusion of the salt molecules. The density distribution is kept approximately stable by using salt gradient protection system. This was a passive system based on the natural circulation of water caused by density difference, as it was first proposed by Akbarzadeh and MacDonalds [25]. In he various study, similar protection systems were used successfully in SPs experiments [26, 27].

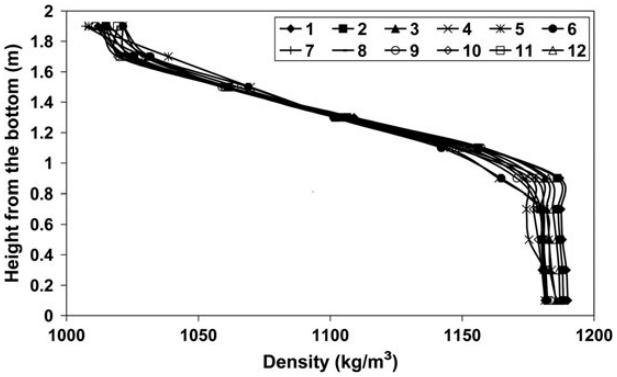


Figure 2. *Density distribution of the ISP.*

Downloaded from https://academic.oup.com/ijlct/article/9/1/45/665396 by Cukurova University user on 05 February 2022

The density difference at low temperature takes place approximately in linear relationship between density and salinity [28]. We used an empirical correlation as given in Equation (5) and calculated our SP zones' salinity. Figure 3 shows a change of salinity in the ISP.

$$s = \frac{\rho - 998.24}{0.756} \tag{5}$$

where s is the salinity (g/kg) and ρ is the density (kg/m^3).

The specific heat capacity of the SP zones is calculated using an emprical equation as given in Equation (10) in [28]. Figure 4 in this regard shows the change of heat capacity of the ISP zones.

$$C = (-0.0044s + 4.1569)1000 \tag{6}$$

where C is heat capacity (J/kg°C).

Figure 5 shows the experimental temperature distributions of the ISP and its surrounding air as measured throughout the year. These experimental temperatures were in fact measured on hourly basis by a data acquisition system. Figure 5a–l shows the daily temperature variations of the inner zones and surrounding air temperatures during the months for the ISP. The average temperature distributions for inner zones of the ISP are determined by using experimental data throughout the year.

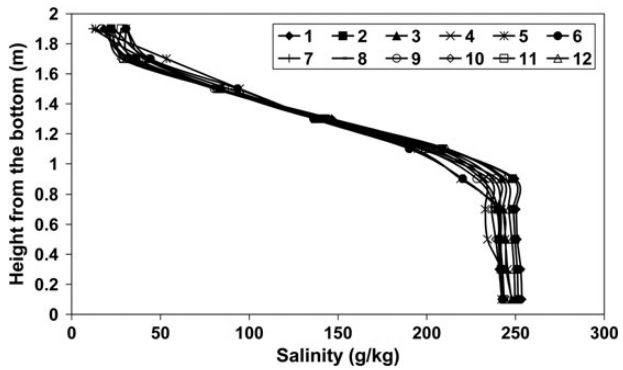


Figure 3. *Salinity of the ISP.*

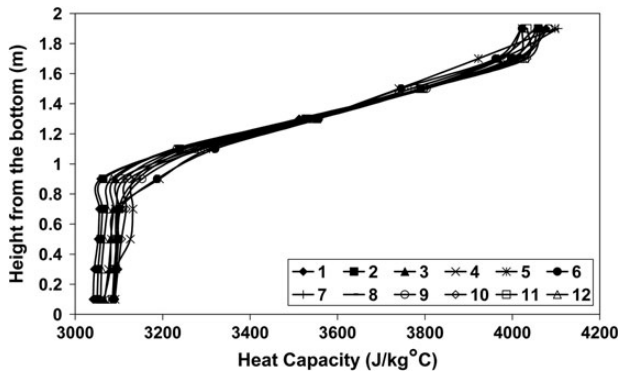


Figure 4. *Heat capacity of the ISP's zones.*

The average temperature distribution of the conventional SP is determined by using the experimental data of an earlier year for the same period. The zones temperatures were measured throughout the month, and monthly average temperature values were obtained at the respective points in Figure 6. It is clear that the zone temperatures vary on monthly basis, depending on the surrounding air temperature and incoming solar radiation for the zones. The temperatures of the zones generally increase with increasing incoming incident solar energy per unit area of surface. There are heat losses taking place from each zone, which become largest in the storage zone as it affects the storage performance drastically. It is important to deal with this zone to improve the performance and hence increase the efficiency of the ISP. Thus, the losses should be minimized, the number of collectors should be increased and a high-efficiency heat exchanger for HSZ and an effective hot-water flow from flat-plate collectors to the heat exchanger in the HSZ by using a circulation pump.

Figure 6 provides a comparison of the temperature distribution of the conventional SP and ISP. Especially in Figure 6, it is shown that the temperatures of the HSZ and NCZ are increased significantly by using solar collectors, but less in UCZ, because the heat exchanger system is placed in the HSZ. First, for the conventional SP, the temperature of the UCZ is observed to peak at 30.33°C in August, and drop as low as 10.40°C in January. Similarly, the temperature of the NCZ is observed to peak 40°C in August, and drop as low as 12°C in January. While the temperature of the HSZ is observed to be maximum at 42°C in August and minimum at 16°C in January. Secondly, for the ISP; the temperature of the UCZ is observed to be maximum at 34°C in August, a minimum at 12°C in January. Similarly, the temperature of the NCZ is determined to be maximum at 47.5°C in September and minimum at 18°C in January, whereas the temperature of the HSZ is measured to be a maximum at 52°C in July and minimum at 18°C in January. As expected, a significant increase in the temperature distributions of the ISP is obtained by using flat-plate collectors.

Note that a significant amount of incident solar radiation is absorbed by the HSZ, and a very small solar radiation is reflected from the bottom wall of the pond. Increasing shading area from top to bottom of the pond allows less solar radiation to pass through and decreases the thermal potential of the pond and, hence, its performance is decreased. Therefore, we analyze the heat storage capacity to compare with energy efficiency of SP and ISP to investigate the performance. The performance of the thermal energy storage depends on the total radiation reaching the pond's HSZ. The best performance of the HSZ of the conventional SP and ISP can be usefully determined by using energy efficiencies. However, in a SP, the stored energy is very low when compared with the solar radiation falling on the surface of zones, so that the efficiencies are also very low. The efficiencies are low in part due to the low

Downloaded from https://academic.oup.com/ijlct/article/9/1/45/665396 by Cukurova University user on 05 February 2022

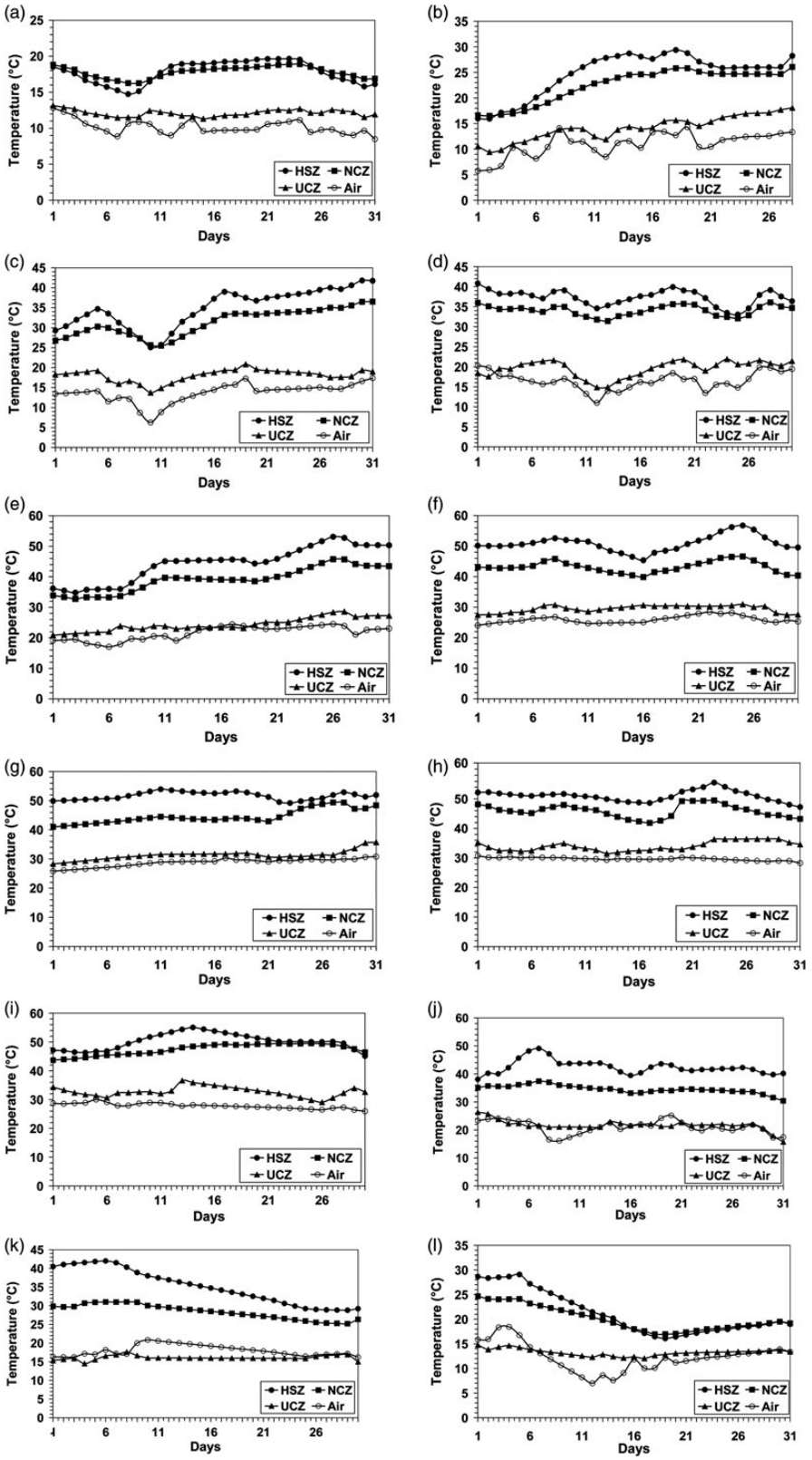


Figure 5. *Daily temperature variations in the zones of ISP and air for (**a**) January, (**b**) February, (**c**) March, (**d**) May, (**e**) June, (**f**) July, (**h**) August, (**i**) September, (**j**) October, (**k**) November and (**l**) December.

Downloaded from https://academic.oup.com/ijlct/article/9/1/45/665396 by Cukurova University user on 05 February 2022

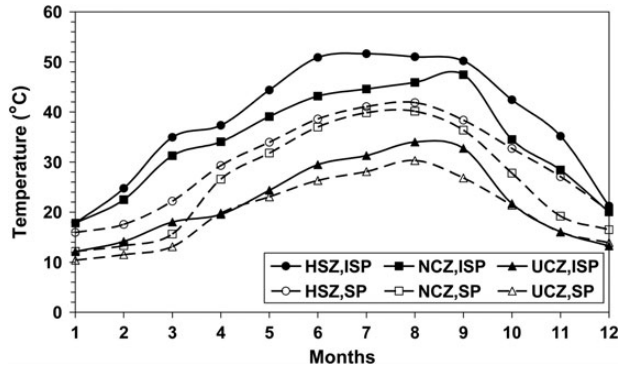


Figure 6. *Comparison of temperature distributions in the zones for both ISP and SP.*

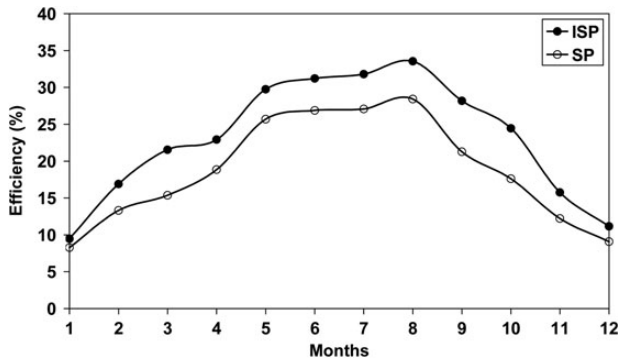


Figure 7. *Comparison of energy efficiencies for both ISP and SP.*

thermal conductivity of the pond filled with salty water. The efficiencies are dependent primarily on the temperature of the salty water and ambient air. The monthly averages of hourly temperatures, net surface area of the zones, transmitted solar radiation to the layers and the thermal energy absorption by the HSZ are calculated. This study in particular provides an important illustration of the effects of shading, side wall, absorption capability, transmission of solar radiation and the thicknesses of the zones on the system efficiency. The results for SP and ISP are then determined and compared.

The energy efficiency profiles for the conventional SP and ISP during a year are given in Figure 7. The maximum efficiencies of the convetional SP and ISP are seen to obtained in August and the minimum efficiencies in January. For the conventional SP, the efficiency is determined to be an average maximum of 28.41% in August and an average minimum of 8.28% in January. Similarly, the corresponding efficiency for the ISP is observed to be a maximum of 33.55% in August and a minimum of 9.48% in January, respectively.

5 CONCLUSIONS

In this article, the energetic performance of the ISP and non-ISP is studied through energy efficiency analysis and the results of SP and ISP are compared for various cases under parametric studies. Energy efficiencies are developed for the HSZ of the ISP through energy balance equations. The energy efficiencies determined for two types of SPs using the experimental data are compared with each other to understant the effect of integration of flat-plate collectors on the performance of the system. As expected, the energy efficiencies of the ISP are found to be higher than the coresponding efficiencies of the non-ISP with large differences in both NCZ and HSZ. High energy efficiencies of the ISP are obtained by connecting some of the collectors to the HSZ. This result helps to promote such ISP systems for practical applications.

ACKNOWLEDGEMENTS

The authors acknowledge the support provided by University of Cukurova in Turkey (Grant No: FEF 2004 BAP4, FEF 2009 D2 and FEF 2010 BAP5), the Council of Higher Education in Turkey and University of Ontario Institute of Technology in Canada.

REFERENCES

[1] Dincer I, Rosen MA. A worldwide perspective on energy, environment and sustainable development. *Int J Energy Res* 1998;**22**:1305–21.
[2] Dincer I, Rosen MA. *Thermal Energy Storage: Systems and Applications*. John Wiley and Sons, New York, 2011.
[3] Karakilcik M, Kıymac K, Dincer I. Experimental and theoretical temperature distributions in a solar pond. *Int J Heat Mass Transf* 2006;**49**:825–35.
[4] Karakilcik M, Dincer I, Rosen MA. Performance investigation of a solar pond. *Appl Therm Eng* 2006;**26**:727–35.
[5] Karakilcik M, Dincer I. Exergetic performance analysis of a solar pond. *Int J Therm Sci* 2008;**47**:93–102.
[6] Ouni M, Guizani A, Lu H, *et al*. Simulation of the control of a salt gradient solar pond in the south of Tunisia. *Sol Energy* 2003;**75**:95–101.
[7] Mansour RB, Nguyen CT, Galanis N. Transient heat and mass transfer and long-term stability of a salt-gradient solar pond. *Mech Res Commun* 2006;**33**:233–49.
[8] Velmurugan V, Srithar K. Prospects and scopes of solar pond: a detailed review. *Renew Sustain Energy Rev* 2008;**12**:2253–63.
[9] Garnier C, Currie J, Muneer T. Integrated collector storage solar water heater: temperature stratification. *Appl Energy* 2009;**86**:1465–9.
[10] Skeiker K. Optimum tilt angle and orientation for solar collectors in Syria. *Energy Conver Manage* 2009;**50**:2439–48.
[11] Sopian K, Alghoul MA, Alfegi EM, *et al*. Evaluation of thermal efficiency of double-pass solar collector with porous–nonporous media. *Renew Energy* 2009;**34**:640–5.
[12] Vargas JVC, Ordonez JC, Dilay E, *et al*. Modeling, simulation and optimization of a solar collector driven water heating, absorption and cooling plant. *Sol Energy* 2009;**83**:1232–44.
[13] Vestlund J, Ronnelid M, Dalenback J. Thermal performance of gas-filled flat plate solar collectors. *Sol Energy* 2009;**83**:896–904.
[14] Dah MMO, Ouni M, Guizani A, *et al*. The influence of the heat extraction mode on the performance and stability of a mini solar pond. *Appl Energy* 2010;**87**:3005–10.

Downloaded from https://academic.oup.com/ijlct/article/9/1/45/665396 by Cukurova University user on 05 February 2022

[15] Li N, Yin F, Sun W, *et al*. Turbidity study of solar ponds utilizing seawater as salt source. *Sol Energy* 2010;**84**:289–295.
[16] Tundee S, Terdtoon P, Sakulchangsatjatai P, *et al*. Heat extraction from salinity-gradient solar pond using heat pipe heat exchangers. *Sol Energy* 2010;**84**:1706–16.
[17] El-Sebaii AA. Thermal performance of a shallow solar-pond integrated with a baffle plate. *Appl Energy* 2005;**81**:33–53.
[18] El-Sebaii AA, Ramadan MRI, Aboul-Enein S, *et al*. Thermal performance of a single-basin solar still integrated with a shallow solar pond. *Energy Convers Manage* 2008;**49**:2839–48.
[19] Velmurugan V, Srithar K. Solar stills integrated with a mini solar pond-analytical simulation and experimental validation. *Desalination* 2007;**216**:232–241.
[20] Velmurugan V, Pandiarajan S, Guruparan P, *et al*. Integrated performance of stepped and single basin solar stills with mini solar pond. *Desalination* 2009;**249**:902–9.
[21] Velmurugan V, Mandlin J, Stalin B, *et al*. Augmentation of saline streams in solar stills integrating with a mini solar pond. *Desalination* 2009;**249**:143–9.
[22] Akbarzadeh A, Johnson P, Singh R. Examining potential benefits of combining a chimney with a salinity gradient solar pond for production of power in salt affected areas. *Sol Energy* 2009;**83**:1345–59.
[23] Hawlader MNA. The influence of the extinction coefficient on the effectiveness of solar ponds. *Sol Energy* 1980;**25**:461–4.
[24] Bryant HC, Colbec I. A solar pond for London. *Sol Energy* 1977;**19**:321.
[25] Akbarzadeh A, MacDonald RWG. Introduction of a passive method for salt replenishment in the operation of the solar ponds. *Sol Energy* 1982;**29**:71–6.
[26] Karakilcik M. Determination of the performance of an insulated prototype solar pond. Ph.D. Thesis. Cukurova University 1998 (in Turkish).
[27] Bozkurt I. Performance investigation of having an insulation and cover cylindrical model solar pond. MSc. Thesis. Cukurova University. 2006 (in Turkish).
[28] Sun H, Feistel R, Koch M, *et al*. New equations for density, entropy, heat capacity, and potential temperature of a saline thermal fluid. *Deep-Sea Res I, Oceanogr Res Pap* 2008;**55**:1304–10.

Downloaded from https://academic.oup.com/ijlct/article/9/1/45/665396 by Cukurova University user on 05 February 2022